

pubs.acs.org/journal/ascecg Research Article

Role of CO₂ and Glycerol in the Formation of Urchin-Like Strontium Carbonate Particles

Alireza Ghorbani, Vitaliy Yurkiv, Josué M. Gonçalves, Azadeh Amiri, Timothy G. Ritter, Mahmoud Tamadoni Saray, and Reza Shahbazian-Yassar*



Cite This: ACS Sustainable Chem. Eng. 2024, 12, 3185-3195



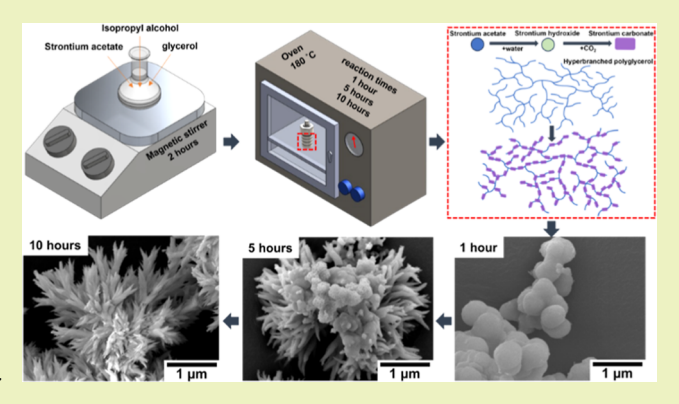
ACCESS I

III Metrics & More

Article Recommendations

s Supporting Information

ABSTRACT: Green synthesis of micro/nanomaterials, using glycerol as a sustainable solvent, offers environmentally and health-friendly pathways. Glycerol's versatility in a solvothermal synthesis is effective for nanoparticle production, yet its mechanistic role in carbonate material formation is unexplored. This study investigates urchin-like strontium carbonate formation via a glycerol-mediated solvothermal synthesis, employing in situ transmission electron microscopy (in situ TEM), scanning electron microscopy, density function theory (DFT), scanning transmission electron microscopy, and X-ray diffraction. In situ TEM observations unveil the initial stages of strontium hydroxide nucleation and subsequent growth as an intermediate phase. The findings suggested that the hyperbranched polymerization of



glycerol plays a pivotal role in the formation of urchin-like morphology. Furthermore, the synergistic effect of glycerol and CO_2 is proposed as the primary driver for the formation of strontium carbonate. Notably, observations showed a morphological transition from spherical to urchin-like with increasing reaction time. DFT studies proposed glycerol as a coadsorbent, boosting the adsorption energy of CO_2 and directing its interaction with $Sr(OH)_2$ resulting in the stable formation of $SrCO_3$. This research provides valuable insights into the urchin-like strontium carbonate formation in a time-dependent process driven by the polymerization of glycerol and its high reactivity with dissolved CO_2 at elevated temperatures.

KEYWORDS: strontium carbonate, glycerol, urchin-like particles, in situ TEM, CO₂ carbonation

■ INTRODUCTION

Green synthesis of micro/nanomaterials minimizes the risks of environmental pollution and health impacts caused by hazardous chemicals. Green synthesis of nanoparticles focuses on devising alternative, safer, energy-efficient, and less toxic pathways for their production. Green solvents present a safer and more sustainable substitute for conventional solvents, thereby diminishing their adverse effects on environmental and human health. Glycerol, a byproduct of triglyceride transesterification, has been widely used as a green solvent in various fields, such as catalysts, organic synthesis, separations, and materials chemistry. The advantages of glycerol, including low toxicity, cost-effectiveness, abundant availability, and renewability, position glycerol as a valuable alternative to conventional volatile organic solvents. Additionally, glycerol can dissolve both inorganic and organic compounds.

The glycerol-mediated solvothermal method has been used as a green chemistry route to synthesize hierarchical nano/microstructures. The solvothermal synthesis technique involves inducing a chemical reaction or decomposition of the precursor materials in a closed system at high temperatures and pressures in order to form the desired compound directly

from a solution. Different solvents, such as isopropyl alcohol, tethanol, and glycerol, have been used in the solvothermal method for synthesizing the desired material. The other advantage of solvothermal synthesis is that most of the time, the reaction taking place is dependent on time, and by changing the reaction time, scientists would be able to evaluate the morphology and structure of the product over time. Also, low vapor pressure (0.01 Pa at 25 °C) and miscibility in water and most of organic solvents make glycerol an excellent choice for solvothermal synthesis.

Glycerol can be used as an agent to synthesize hierarchical nanoparticles. Zhang et al. investigated the impact of glycerol addition on the synthesis of hierarchical LaCO₃OH using a glycerol-mediated solvothermal method to show that the high concentration of glycerol significantly influences the develop-

Received: November 4, 2023 Revised: January 17, 2024 Accepted: January 19, 2024 Published: February 9, 2024





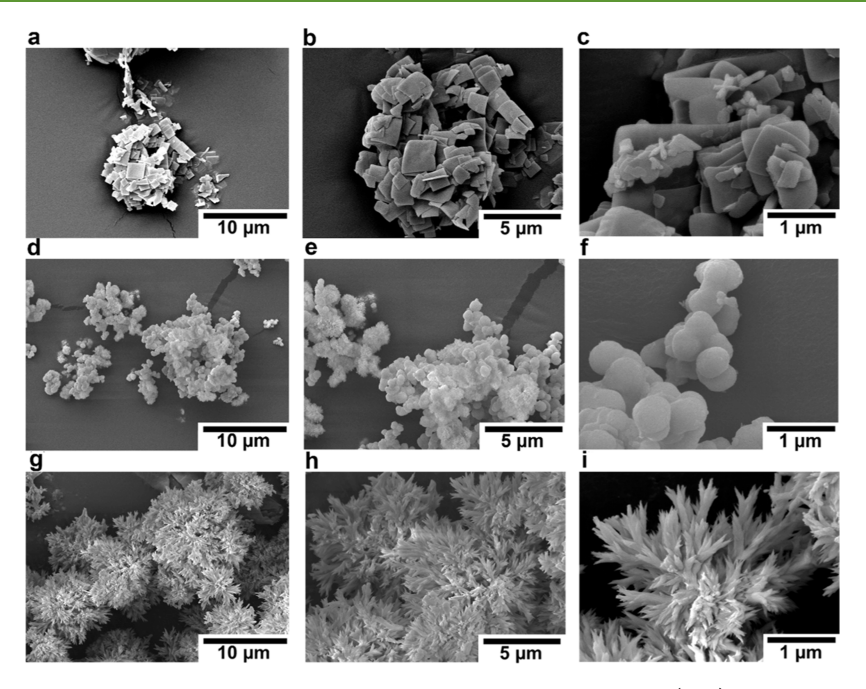


Figure 1. SEM images of solvothermally synthesized materials viewed at different magnifications: (a-c) strontium acetate dissolved in isopropyl alcohol (without glycerol) heated for 10 h at 180 °C in an autoclave, (d-f) synthesized material obtained by the solvothermal mixture of strontium acetate, isopropyl alcohol, and glycerol with 1 h reaction time at 180 °C, and (g-i) with 10 h reaction time at 180 °C.

ment of a plum blossom-like morphology in LaCO₃OH. Additionally, they studied the effect of reaction time on the final morphology of LaCO₃OH revealing a transformation from wire structured into a sphere composed of rods, then progressing to a multifaceted spherical structure, and finally evolving into the distinctive plum blossom-like as the reaction time increased. Wang et al. 14 studied the impact of glycerol concentration on the formation of uniform urchin-like α -FeOOH to show that the concentration of glycerol can be precisely regulated to tailor the structure of the products. They proposed that a lower concentration of glycerol leads to the formation of a solid structure, whereas a higher concentration of glycerol can be employed to synthesize hollow spheres.¹⁴ Wei et al. 15 utilized a template-free glycerol-mediated hydrothermal process with microwave heating to synthesize hollow nest-like α-Fe₂O₃. Their research findings indicated that the presence of glycerol in the solvent led to the crystallization of α-Fe₂O₃ into rod-like nanostructures, where polymerized glycerol potentially acted as a directing agent. Subsequently, these nanorods were assembled on the surface of glycerol droplets, forming a compact shell. The inner glycerol droplet could be easily removed through solvent extraction during the rinsing and drying process resulting in the formation of hollow spheres.15

Multiple studies have indicated that the introduction of polymers during the synthesis of carbonate minerals has a significant impact on both the morphology and crystal structure of the resulting carbonates. ¹⁶ Guo et al. ¹⁷ investigated the combined impact of poly(L-glutamic acid)-b-poly(ethylene glycol)-b-poly(L-glutamic acid) (PEG-b-pGlu) and the solvent combination on the development of calcium carbonate. They showed that the fabrication of vaterite microspheres could be achieved by taking advantage of the synergistic effects of the block copolymer and the solvent mixture. By introducing poly(styrene-alt-maleic acid) as an additive during the synthesis, Xu et al. ¹⁸ successfully acquired calcite mesocrystals

exhibiting a hierarchical pyramidal self-assembly morphology. The study conducted by Yu et al. 19 demonstrated that employing different concentrations of poly(acrylic acid) (PAA) yielded diverse crystal morphologies of calcite, such as, plates, rectangles, ellipsoids, and cubes. Ji et al.²⁰ utilized poly(ethylene glycol) (PEG) and sodium dodecyl sulfate (SDS) as a template for growth of hollow CaCO3 microspheres. Bastakoti et al.²¹ demonstrated that micelles formed by the triblock copolymer poly(styrene-b-acrylic acid-b-ethylene glycol) (PS-b-PAA-b-PEG) could serve as a template for the fabrication of hollow nanosphere CaCO₃. In another study, Yu et al.²² observed that by increasing the concentration of poly(styrene-alt-maleic acid) (PSMA) during the synthesis of SrCO₃, the morphology of carbonate materials changed from bundle-like aggregates to dumbbells and eventually to perfect spherical particles. In their work, Sreedhar et al.²³ illustrated that the organic functional groups present in gum acacia, a natural polymer, interacted with strontium and carbonate ions, leading to a modification in the morphology of strontium carbonate. By employing various concentrations of gum acacia, the researchers successfully obtained a range of morphologies, including rods, flower-like shapes, cross-like structures, doughnut shapes, and rice grain shapes. Xu et al.²⁴ showed that strontium carbonate crystals synthesized with polymers with hydroxyl groups as a regulator exhibited a needle-shaped morphology. Conversely, strontium carbonate crystals synthesized with carboxyl groups as regulators displayed a short-bar morphology.

While it is shown that the presence of polymers (and glycerol) can affect the growth and morphology of SrCO₃, there has been no comprehensive study of the role of glycerol during the formation of strontium carbonate. Glycerol is a great green solvent for synthesizing nanomaterials.²⁵ It is nontoxic, nonflammable, biodegradable, and can mix with water and organic solvents easily.²⁶ Here, we studied the formation of urchin-like strontium carbonate from strontium

glycerolates. A mechanism is proposed for the formation of such a morphology of strontium carbonate in the presence of glycerol and CO_2 . In addition, the effect of reaction time on the morphology of strontium carbonate was studied.

RESULTS AND DISCUSSION

The morphology of the as-synthesized materials was evaluated using scanning electron microscopy (SEM) imaging. Figure 1 shows the SEM images of three batches of specimens prepared by solvothermal synthesis. Figure 1a-c represents the morphology of the specimens without the presence of glycerol. It can be seen that the morphology of these specimens is the agglomeration of plate-like particles, and the high magnification image of these clusters is presented in Figure 1c. Figure 1d-f shows the morphology of solvothermal synthesized specimens in the presence of glycerol at a reaction time of 1 h. As compared with Figure 1a, the morphology of the particles changes from plate-like to spherical due to the presence of glycerol. This shows that adding glycerol affects the morphology of the synthesized particles.²⁷ The effect of the synthesis time on the morphology of particles can be seen in Figure 1g-i. These figures show that the spherical particles shown in Figure 1f are changed to urchin-like particles by increasing the solvothermal synthesis time. It has been found that the size, shape, and morphology have a strong effect on the material properties. 28 Urchin-like strontium carbonate, characterized by its larger surface area and controlled charge distribution, holds promise for diverse applications, such as catalysts, ²⁹ capacitors, ²⁸ and sensors, ³⁰ creating advantageous microenvironments compared to spherical morphology.³¹ Notably, Wang et al.²⁸ demonstrated that the electrochemical performance of urchin-like strontium carbonate surpasses that of spherical counterparts, exhibiting a specific capacitance of 41.7 F·g⁻¹ at a current density of 1 A·g⁻¹ marking a 2.5 times improvement. Additionally, in a study by Fang et al., 30 urchinlike strontium carbonate nanocrystals embedded in collagen films showcased potential applications in flexible piezoelectric sensors. The developed device exhibited a voltage and current of 0.7 V and 80 nA, respectively, under the bending mode, suggesting its suitability for miniature actuators and electronic

It is obvious that the presence of glycerol is the key for the formation of an urchin-like morphology in particles. Interestingly, the reaction time in Figure 1a is the same as in Figure 1i (both 10 h of reactions), but the morphology of the sample has changed from plate-like to urchin-like with addition of glycerol. In recent years, glycerol has become a desired green solvent for the synthesis of nanomaterials. Glycerol is a nontoxic, noninflammable, and biodegradable product of the biodiesel industry. The high boiling point of glycerol (290 °C) makes it a proper choice to use in synthesis with reactions at high temperatures without losing the solvent by evaporation.⁶ Also, low vapor pressure (0.01 Pa at 25 °C) and miscibility in water and most of organic solvents make glycerol an excellent choice for solvothermal synthesis.²⁶ In addition, glycerol is a green solvent that is environmentally friendly, and considering conventional synthesis methods of SrCO₃ mainly using urea, it would be a green replacement.²⁸ Urea has been considered to cause uremia, which is a serious medical condition happening when the urea accumulates in the blood. It also can directly promote cell death and calcification in blood vessels. 2 Cyanate (OCN⁻) is a reactive decomposition of urea (CH_4N_2O) that could cause endothelial dysfunction where the

cyanite reduces the expression of endothelial nitric oxide synthase (an enzyme that produces nitric oxide, a molecule that helps regulate vascular tone and blood flow), and endothelium (i.e., inner lining of blood vessels) is not able to perform its functions such as regulating vascular tone, blood flow, and coagulation.³³ Bone tissue engineering is one of the potentially promising applications of strontium carbonate,³⁴ and changing urea to glycerol in the synthesis of it, could potentially help to have more cytocompatibility and less toxicity of strontium carbonate. Table S2 represents some detailed information on the precursor, solvent, and reagent of strontium carbonate of the solvothermal synthesis of strontium carbonate, compared to our synthesis method. It is interesting to note that the reaction time in most of the other studies on the solvothermal synthesis of strontium carbonate is at least twice³⁵ (in two cases even 4 times^{28,36}) as the time we used in our research. It can be considered that the method of our synthesis will use less energy (compared to other studies) for the fabrication of strontium carbonate by reducing the reaction time of the synthesis.

To gain a better understanding of particle morphology evolution during solvothermal synthesis, the SEM images of solvothermal synthesized particles in the presence of glycerol at reaction times of 30 min and 5 h are presented in Figure S2. Comparing the SEM images of particles obtained after 30 min reaction (Figure S2a) with the ones produced after 1 h reaction time (Figure 1f), we can see a similarity between the morphologies of these two specimens. In addition, the morphology of the sample with a 5 h reaction time resembles the particles with 10 h reaction time, and the only difference is that the number of spherical particles are higher in the sample after 5 h reaction time. There are several studies discussing how glycerol could change the morphology and structure of nanomaterials when used in the synthesis process.²⁷ Metalglycerolates with different morphologies (such as the sphere³⁷ and flower-like³⁸) can be prepared by the reaction of a metal salt with glycerol at elevated temperatures.³⁹ Most of the materials synthesized using glycerol, have a uniformly distributed sphere-like morphology but the type of metal ion, concentration of glycerol, and presence of cosolvent could affect the morphology and structure of these materials.²⁵

On this matter, Kim and Jang⁴⁰ demonstrated that reducing the concentration of glycerol using isopropyl alcohol could favor the growth of hedgehog titanium-glycolate crystals rather than the rod-like shape crystals during a microwave heating process. In another research Li et al., 41 indicated that using glycerol as a solvent (in combination of ethanol and ethyl ether) would result in the formation of mesoporous TiO₂ nanosheet-based hierarchical tubular superstructure as a product of calcination of solvothermally synthesized Tiglycerolate; while using only ethanol and ethyl ether would result in the formation of irregular aggregated pure anatase TiO₂ particles. Zhou et al., 42 studied the effect of solvent on the formation of hierarchical ZnO particles. Using different solvents, such as ethanol, water, and glycerol, in a template-free solvothermal synthesis, they concluded that using glycerol as a solvent will result in the formation of nanosheets and nanoparticles with different shapes and sizes, while using water as a solvent would form irregular-shaped nanosheets and replacing glycerol with ethanol would result in formation of a three-dimensional net structure of interconnected ZnO nanosheets. Yang et al.⁴³ showed that using water as a solvent for the hydrothermal synthesis of Ni(OH)2 would yield only

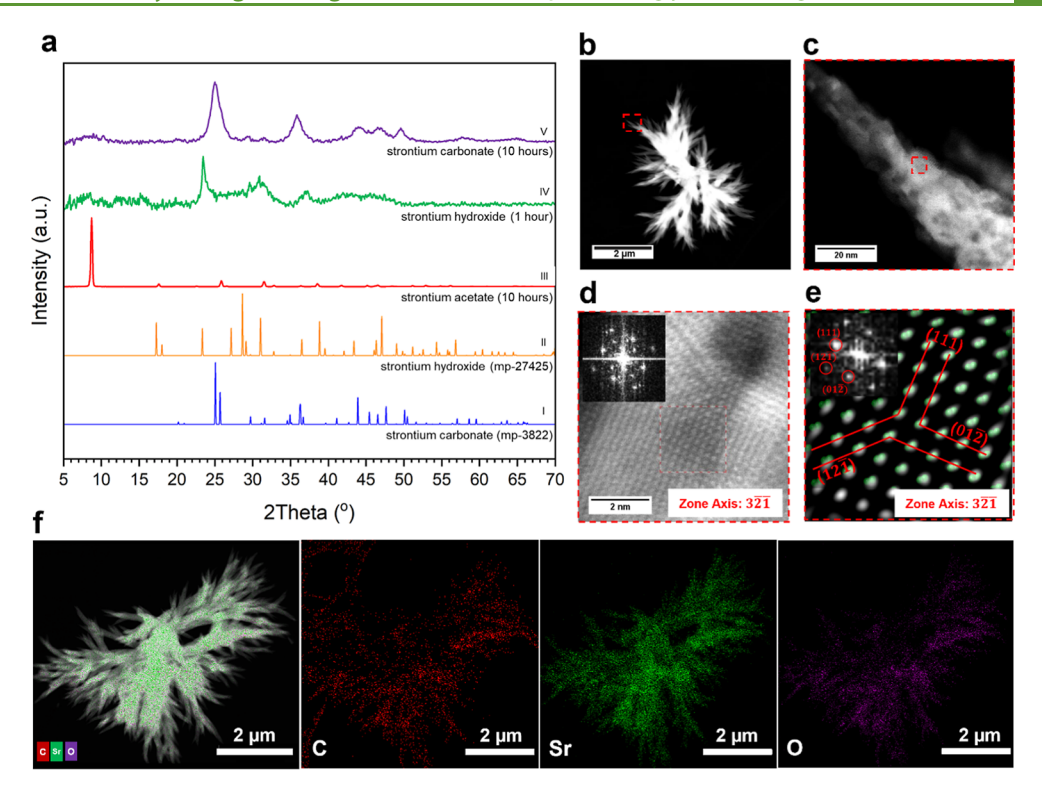


Figure 2. XRD and STEM characterizations of solvothermally synthesized particles in the presence and absence of glycerol. (a) Standard XRD patterns of strontium carbonate [mp-3822] (marked as I), and strontium hydroxide [mp-27425] (marked as II), and XRD results of strontium acetate dissolved in isopropyl alcohol (without glycerol) heated for 10 h at 180 °C in an autoclave (marked as III), solvothermally synthesized product of mixture of strontium acetate, isopropyl alcohol, and glycerol with 1 h reaction time (marked as IV), and solvothermally synthesized product of mixture of strontium acetate, isopropyl alcohol, and glycerol with 10 h of reaction time (marked as V). (b–e) HAADF-STEM images of the material obtained by solvothermal synthesis of mixture of strontium acetate, isopropyl alcohol, and glycerol with 10 h of reaction time with glycerol, and (f) STEM-EDS results of strontium carbonate particles synthesized with glycerol with a reaction time of 10 h.

irregular nanosheets, while adding glycerol to the solvent water at a ratio of 1:23 (glycerol/water) would form $Ni(OH)_2$ carnation-like particles.

In the next step, X-ray diffraction (XRD) was used as the primary bulk characterization approach to study and compare phases formed after synthesis. Figure 2a shows the XRD result for particles obtained by dissolving strontium acetate in isopropyl alcohol without the presence of glycerol and after 10 h of heating at 180 °C in an autoclave. By comparing the patterns in Figure 2a, one can see that the most intense peak $(2\theta \approx 8.5^{\circ})$ in the XRD data (pattern III) of the solvothermally obtained specimen without glycerol is not present in the particles synthesized with glycerol after 1 and 10 h of reaction time (patterns IV and V). Figure 2a (I,II) represents the standard XRD patterns of strontium carbonate and strontium hydroxide, respectively. Figure 2a(IV) showcases the XRD result for particles synthesized after 1 h of reaction in an autoclave at 180 °C. Figure 2a (III) showcases the XRD result for solvothermal synthesized particles after 10 h at 180 °C. The XRD peaks for particles synthesized after 10 h are in good accordance with the XRD pattern of orthorhombic strontium carbonate, 44 as the main peaks of orthorhombic strontium carbonate are present in the 2θ = 25.2, 29.7, 31.6, 36.3, 41.5, 44.2, 46.8, 50.1, and 63.9°, which are assigned to the planes (111), (002), (012), (112), (220), (221), (202), (113), and (312), respectively, similar to pure orthorhombic strontianite, a natural mineral of strontium carbonate [mp-3822]. It is important to note that the XRD result of sample with 1 h reaction time has the most major

peaks of orthorhombic strontium hydroxide [mp-27425] and only the two peaks near 17° are missing [these peaks represent planes (011) and (002), respectively]. Other main peaks at 2θ = 23.3 (012), 27.1 (110), 28.6 (111), 29.1 (102), 31.0 (013), 31.1 (021), 38.8 (121), and 47.1 (123) can be characterized in the XRD pattern. Notably, the two peaks are missing, and the most intense peak has been changed from (111) to (012). This can be assigned to the preferred orientation of strontium hydroxide particles, and also, due to the morphology of the samples (urchin-like) it seems reasonable to have the preferred orientation.⁴⁵ The other phenomenon happening here is peak broadening, which can be a result of having finer particles and residue of organic materials (such as polyglycerol) after the washing process.⁴⁶ The XRD pattern of sample with 5 h reaction time is shown in Figure S3. Analyzing this pattern shows the major peaks at $2\theta = 25.2$ and 36.3° that can be assigned to the (111) and (112) planes of the strontium carbonate [mp-3822] and reveals that after 5 h of reaction, the main phase has changed from strontium acetate to strontium carbonate.

The detection of strontium carbonate instead of strontium glycerolate is interesting. One of the main characteristics of glycerolate materials is the XRD peak at around $2\theta=10^{\circ},^{47}$ which is not present in the XRD pattern of strontium carbonate. Also, the XRD pattern of strontium carbonate shows a high degree of crystallinity, while the XRD pattern of most metal-glycerolate materials has no major peaks except an intense peak at $2\theta=10^{\circ}$. There are several reports in the literature showing that under similar solvothermal synthesis

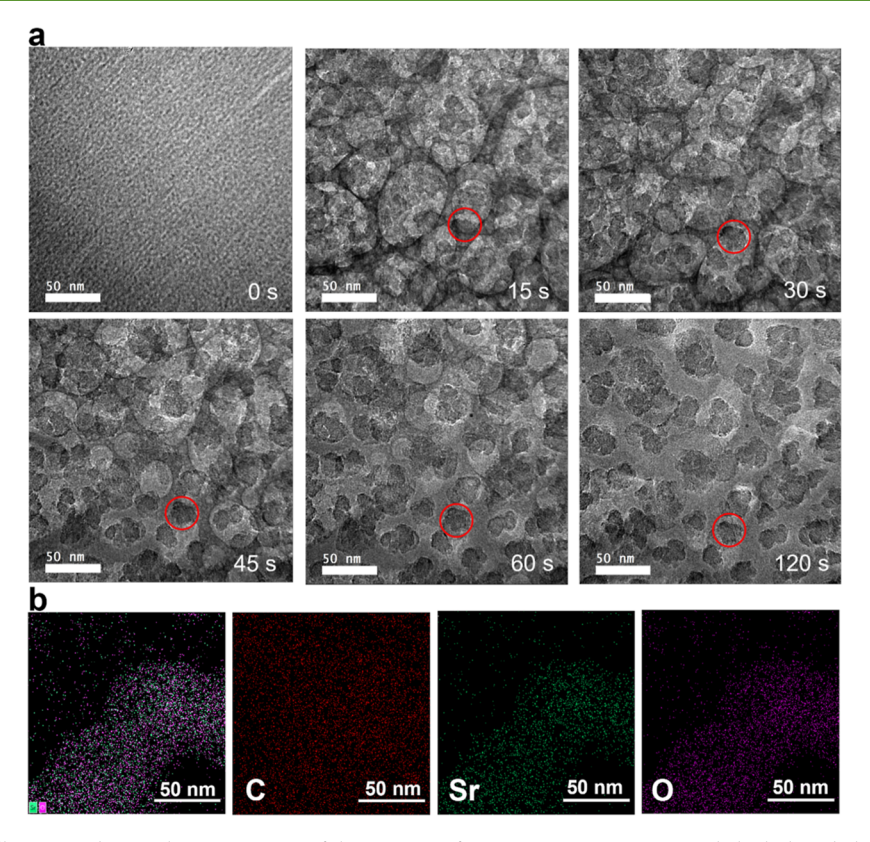


Figure 3. In situ liquid cell TEM and EDS characterization of the mixture of strontium acetate, isopropyl alcohol, and glycerol: (a) time-dependent in situ GLC-TEM images of nucleation and growth of strontium hydroxide (the red circle demonstrates an example of the particles that are forming and growing under the electron beam) and (b) EDS results collected from a nanoparticle of strontium hydroxide.

conditions metal glycerolates from Ni,⁴⁸ Fe,⁴⁹ Mn,⁵⁰ and Zn⁵¹

In order to better clarify the role of glycerol on the crystalline phase of solvothermally prepared specimens, the XRD data of as-received strontium acetate and strontium acetate dissolved in isopropyl alcohol (without glycerol) after 10 h of heating at 180 °C in an autoclave are shown in Figure S4. The results show that in the absence of glycerol, the reaction led to the formation of strontium acetate, and although some small peaks in the XRD pattern of specimen without glycerol can be related to the strontium carbonate, most of the peaks are exactly similar to the XRD pattern of asreceived strontium acetate, showing that synthesis in such a condition (with no added glycerol) would not form the strontium carbonate.

In the next step, the hydrothermally synthesized particles were studied by scanning transmission electron microscopy (STEM) and energy-dispersive spectroscopy (EDS) to gain a better understanding of their local chemistry and phase structure. The high-angle annular dark field (HAADF) images of the specimen after 10 h of reaction time in the presence of glycerol are shown in Figure 2b-d. Figure 2b,c demonstrates the urchin-like structure of the strontium carbonate, which can be seen in the SEM images (Figure 1i). The high-resolution STEM-HAADF image of the selected area in Figure 2c and the corresponding FFT spectra confirm the polycrystalline nature of the formed branches (Figure 2d). This finding contradicts earlier studies⁵² that suggested the single-crystalline nature of needle-shaped strontium carbonate due to a directional growth mechanism. Additionally, the dashed-line box highlights a single crystalline domain with atomic columns in the [321]

zone axis (Figure 2d). Figure 2e shows the FFT and inverse FFT images of the dashed line box in Figure 2d. The FFT and IFFT patterns indicate (111), (01 $\overline{2}$), and (12 $\overline{1}$) planes of strontium carbonate in the [32 $\overline{1}$] zone axis.

Subsequently, STEM-EDS was used for identifying the composition and elemental distribution of strontium carbonate specimens. Figure 2f shows the elemental distribution of particles synthesized after 10 h of solvothermal reaction in the presence of glycerol. The distribution of oxygen and carbon are in good agreement with the distribution map of strontium indicating that the particles are made of strontium, carbon, and oxygen. These maps were collected from specimens distributed on a lacy carbon grid explaining why carbon is present in areas outside of particles.

In order to study the initial growth steps of strontium hydroxide particles, in situ TEM was used in this research. In situ graphene liquid cell (GLC)-TEM has become an essential tool for imaging the nucleation and growth of particles at the nanoscale.⁵³ As seen in the time-lapsed TEM data (Figure 3a and Video S1), the solution of strontium acetate, isopropyl alcohol, and glycerol at the starting point (t = 0 s) showed no obvious formation of particles. Under electron beam irradiation, some small size nuclei precipitated where one is highlighted with a red circle at t = 15 s. These particles are initially small but over time, they grow and become larger (marked with the red circle during the time frames of 15 to 120 s). The morphology of these particles is consistent with the particles that interact with polyglycerol to form polymertemplated strontium carbonate. As can be seen, the size of particles is increasing, while the number of particles is decreasing. This indicates the agglomeration of early-stage

Figure 4. DFT calculation results illustrating the formation of $SrCO_3$ (central image) from the initial adsorbate structure of glycerol and CO_2 over the $(3\overline{21})$ surface of $Sr(OH)_2$ (left). The far-right image illustrates obtained electron density of optimized structure further proving the formation of $SrCO_3$ as a result of CO_2 interaction with the $Sr(OH)_2$ surface. The gray spheres represent carbon atoms, the red spheres are oxygen atoms, the white spheres are hydrogen atoms, and the green spheres are Sr atoms.

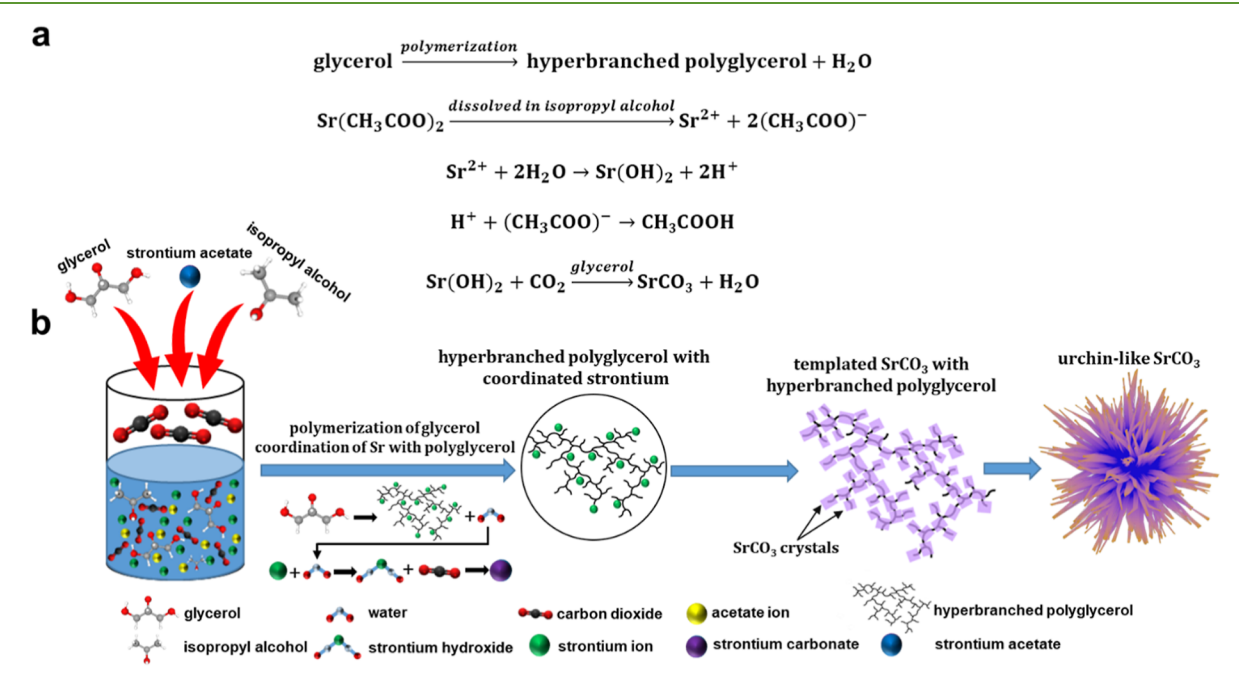


Figure 5. Proposed reaction pathway for the strontium carbonate formation: (a) chemical reactions involving the formation of hyperbranched polyglycerol and conversion of strontium acetate to strontium carbonate and (b) schematic demonstration of the formation and growth of urchin-like strontium carbonate.

particles to form larger irregular-shaped particles that could be a transient stage of the nucleation and growth of the intermediate phase, i.e., strontium hydroxide. Also, it is interesting to mention that the morphology of the formed particles during the in situ GLC microscopy appears as assembly of the particles in the matrix of glycerol. It is speculated that the e-beam irradiation could trigger the polymerization process of glycerol, and the formed polyglycerol could interact with strontium particles to form an assembly similar to the initial steps of urchin-like strontium carbonate fabrication.

To confirm the formation of strontium hydroxide during the in situ GLC-TEM imaging, the EDS maps were collected from the particles. The EDS maps in Figure 3b show that in areas where strontium is detected, oxygen is also present and the signals of C are coming from the grid. This suggests that during the in situ GLC TEM imaging, strontium hydroxide particles form, and become insoluble in the solution. The atomic percentage values of elements calculated using the STEM-EDS spectrum and the spectrum are shown in Figure S5. The results of the EDS spectrum show that the at. % of carbon, oxygen, and strontium are 77.1, 16.8, and 6.1%, respectively. These atomic percentages could match with the composition of $Sr(OH)_2$ because the ratio of O and Sr in the

EDS spectrum is around 2.75. Considering that the TEM grids have a carbon support, the atomic percentage calculated for carbon is not reliable for quantification.

The formation of strontium carbonate during the solvothermal synthesis was puzzling considering there is significant body of literature on metal glycerolates produced under similar conditions.⁴⁷ In order to verify the formation of metal glycerolates under the synthesis conditions leading to strontium carbonate particles, zinc glycerolate materials were synthesized by dissolving 2.5 mmol of zinc acetate in IPA and glycerol and keeping the reaction at 180 °C in an autoclave for 10 h. The results confirmed the formation of Zn-glycerolate and are discussed in the Supporting Information document. It is interesting that strontium acetate under a hydrothermal synthesis with glycerol forms strontium carbonate but zinc acetate under exact synthesis conditions form Zn-glycerolate. This observation points to the high reactivity of Sr with other species and is discussed later in this work (Figure 4).

Proposed Pathway for the Formation of Strontium Carbonate. Here, we propose a pathway for the nucleation and growth of strontium carbonate in this solvothermal process (Figure 5a,b). This mechanism consists of two steps, and glycerol plays a major role in that process. Initially, it is important to mention that glycerol can undergo the polymer-

ization process at reaction conditions (10 h in 180 °C)^{54,55} forming hyperbranched polyglycerol (HB-PG). This is known as polyglycerolation, where glycerol can be converted into hyperbranched polyglycerol. This process is typically done using a catalyst, such as dolomite (CaO·MgO), 56 Ca(OH)₂, 57 and acetic acid,⁵⁸ and a high temperature (between 100 and 240 °C) and reduced pressures (between 26 kPa to atmosphere). 59 During polyglycerolation, the catalysts facilitate the addition of multiple glycerol molecules to a growing polyglycerol chain. This results in a hyperbranched structure, with multiple branches coming off the main chain. The degree of branching can be controlled by adjusting the reaction conditions, such as the reaction temperature, pressure, and the type and amount of catalyst used. 60 Acetate ions can be used as a catalyst in the polyglycerolation of glycerol to form hyperbranched polyglycerols. Acetate ions can act as a Lewis base catalyst, which means that it can donate a pair of electrons to the glycerol molecule and form a complex with the intermediate in the reaction.⁶¹ This complex can then undergo a nucleophilic attack on glycerol, leading to the formation of a glycerol molecule with an ester bond to the acetate ion. This process can be repeated multiple times, leading to the formation of a hyperbranched polyglycerol.⁵⁸

Also, it is important to note that the polymerization of glycerol produces water. 62 Once strontium acetate, Sr(CH₃ CO₂)₂, is dissolved in isopropyl alcohol, it can be dissociated into ions of strontium and acetate. In the next step, strontium ions react with water, produced from the polymerization process of glycerol, and the product of this reaction is expected to be strontium hydroxide and hydrogen ions.⁶³ Then, the strontium hydroxide is likely to produce strontium carbonate in a reaction with dissolved carbon dioxide.⁶⁴ The air contains around 0.04% carbon dioxide, and during the synthesis this carbon dioxide is dissolved in the stirring solution of strontium acetate, isopropyl alcohol, and glycerol (the solubility of carbon dioxide in isopropyl alcohol at room temperature and atmospheric condition is around 1400 ppm and the solubility of carbon dioxide in glycerol at standard temperature and pressure (STP) conditions is 133,000 ppm).65 Previous research showed that strontium hydroxide can react with CO₂ from the environment and form strontium carbonate. 66 It is worth mentioning that strontium hydroxide is a known adsorbent of carbon dioxide forming strontium carbonate after adsorption of CO₂. 52,67 This reaction is likely to happen in our synthesis condition because the formation of strontium carbonate from strontium hydroxide and carbon dioxide is thermodynamically favorable ($\Delta G^{\circ} = -4.4 \text{ kJ/mol}$ in room temperature).⁶⁸ After the formation of strontium carbonate particles, the presence of hyperbranched polyglycerol within the SrCO₃ acts as a template matrix for the material to form the urchin-like strontium carbonate.

A comprehensive DFT study was conducted to understand the conversion of strontium hydroxide to strontium carbonate in the presence of glycerol and CO_2 . Following the above presented experimental results (cf., Figure 2), we have created $(3\overline{21})$ Sr(OH)₂ and SrCO₃ surfaces from the unit cell of a corresponding compound, as shown in Figure S9. Consequently, glycerol and CO_2 interactions over those surfaces were studied using DFT calculations. Figure 4 shows the DFT computational outcomes, illustrating both the initial and optimized configurations of a glycerol molecule accompanied by three proximate CO_2 molecules on the $(3\overline{21})$ surface of Sr(OH)₂. In the initial atomic configuration (left-most image

in Figure 4), the individual molecules of glycerol and three CO₂ are randomly placed, while the central picture showcases their optimized positions obtained in the present DFT. It could be clearly observed that the formation of SrCO₃ for the two CO_2 molecules' interaction with $Sr(OH)_2$, while the one CO₂ in the background does not lead to SrCO₃ formation and , however, still strongly adsorbs over the surface. Furthermore, the right-most image, with its superimposed electron density contours, provides compelling evidence of the formation of $SrCO_3$ on the $Sr(OH)_2$ surface. Upon adsorption of CO_2 onto the Sr(OH)₂ surface in the vicinity of glycerol, the resultant formation of SrCO3 is observed. This transformation is not only supported by the optimized structural alignment but is further corroborated by the electron density distribution, as illustrated in Figure 4 (right-most image). The discernible electron density patterns around the Sr-O-C bonds, in particular, substantiate the formation of SrCO₃.

The implication of this $SrCO_3$ formation from $Sr(OH)_2$ is profound. It suggests a potential mechanism wherein the $Sr(OH)_2$ surface, in the presence of glycerol, can facilitate the capture and conversion of CO_2 , thereby forming stable carbonate structures. This observation paves the way for potential applications in CO_2 capture and sequestration methodologies, leveraging the $Sr(OH)_2$ substrate's ability to engage and immobilize CO_2 molecules effectively. Furthermore, the role of glycerol as a mediating molecule in this process offers intriguing avenues for further exploration, particularly in enhancing the efficiency and specificity of the CO_2 conversion on metal hydroxide surfaces.

We have further studied glycerol and the interaction of CO₂ with the Sr(OH)₂ surface separately. Panel (a) of Figure S10 demonstrates the initial configuration of a glycerol molecule absorbed alone onto the $Sr(OH)_2$ (321) surface and its corresponding optimized configuration. Notably, the optimization retains the adsorbed position of glycerol, suggesting a stable interaction. This stability is further underscored by the electron density plots on the right, revealing a significant overlap in regions around the glycerol molecule and the Sr(OH)₂ surface atoms, indicating strong bonding interactions. In contrast, panel (b) of Figure S10 showcases the adsorption dynamics of CO_2 on the $(3\overline{21})$ surface of $Sr(OH)_2$. The initial configuration depicts the CO2 molecule in proximity to the surface, but the subsequent optimized configuration suggests desorption of CO₂, reverting it to the gas phase. This highlights the inherently unstable nature of the adsorption of CO_2 on the $Sr(OH)_2$ (321) surface in the absence of glycerol.

To confirm the role of carbon dioxide in the formation of strontium carbonate, a control experiment was conducted. In this experiment, argon bubbling was used while the solution of strontium acetate, isopropyl alcohol, and glycerol was stirred. This was done to minimize the dissolution of carbon dioxide in the solution. Then, the solution was placed in an oven at 180 °C for 10 h. The selected area diffraction (SAD) pattern is then used to measure the d-spacings of the crystals in the produced powders. The SAD patterns of strontium compound (synthesized without CO₂) and strontium acetate (as-received precursor salt) are compared in Figure S6. The results show that the sample without CO_2 has most of the *d*-spacings (=3.9, 3.6, 3.2, 2.7, 2.5, 2.0, 1.9, 1.8, 1.7, and 1.4 Å) that can be found in the as-received strontium acetate. This confirms that carbon dioxide plays a significant role in formation of strontium carbonate during the hydrothermal synthesis.

Evidently from Figures 4 and S10, the adsorption of CO_2 on the $Sr(OH)_2$ surface results in the formation of $SrCO_3$ occurring only when glycerol is present. This hints at a potential catalytic or facilitative role played by glycerol in promoting the chemisorption of CO_2 and its subsequent reaction with $Sr(OH)_2$ to form $SrCO_3$. To elucidate further, glycerol could be functioning as a coadsorbent or catalyst, enhancing the adsorption energy or providing necessary active sites for CO_2 , thus facilitating its interaction with $Sr(OH)_2$ and culminating in the stable formation of $SrCO_3$. Analyzing the electron density obtained in the present DFT calculations, it could be concluded that the presence of glycerol on the $Sr(OH)_2$ surface induces polarization effects, leading to charge redistribution. This can enhance the electrostatic attraction between CO_2 and the surface, facilitating $SrCO_3$ formation.

We believe the formation of strontium hydroxide is the outcome of glycerol polymerization, where water is produced as a byproduct. This explains the preference for strontium acetate instead of strontium carbonate when glycerol is not present in the solution medium. This is confirmed by the XRD results obtained from particles when strontium acetate was dissolved in isopropyl alcohol and subjected to hydrothermal synthesis of 10 h at 180 °C. As seen in Figure 2a(I), the XRD peaks match well with strontium acetate phase and only a minor phase of strontium carbonate was detected.

We have compared the interaction of glycerol and CO_2 over the $Sr(OH)_2$ surface with the corresponding interaction over the $SrCO_3$ ($3\overline{21}$) surface. Figure S11 illustrates the DFT results of one glycerol and one CO_2 molecule adsorbates stability over the $SrCO_3$ surface. Similar to the results of the $Sr(OH)_2$ surface (cf., Figure 4), the left atomic arrangement shows the initial configuration, where both glycerol and CO_2 tightly positioned on the surface of $SrCO_3$, while the right image illustrates the optimized structure. As can be observed, optimization leads to the slight desorption of both molecules, indicating a metastable configuration of adsorbates over the $SrCO_3$ surface. These results indicate that $SrCO_3$ is more thermodynamically stable and cannot be further transformed as in the case of $Sr(OH)_2$.

To gain further insights about the experimentally observed phenomena, we conducted AIMD simulations to investigate the behavior of glycerol over the $Sr(OH)_2$ surface. The AIMD simulations were performed for 500 fs at 393 K placing one molecule of glycerol over the $(3\overline{21})$ $Sr(OH)_2$ surface. We aimed to observe if CO_2 can be formed from the glycerol interaction over the $Sr(OH)_2$ surface. The AIMD simulation results (Figure S12) show that glycerol is likely not to dissociate over the $Sr(OH)_2$ surface even at elevated temperatures. This indicates that CO_2 from air might indeed be adsorbed over the surface leading to $SrCO_3$ formation, while glycerol acts as a mediator.

We found only one prior work on the synthesis of strontium glycerolate ⁶⁹ confirming that it may be possible to fine-tune our synthesis procedure for direct synthesis of strontium glycerolate instead of strontium carbonate. However, we should highlight the differences in the synthesis procedure between the current work and the work of Lisboa et al. ⁶⁹ According to Lisboa et al. ⁶⁹ strontium monoglycerolate was synthesized by mixing strontium oxide with glycerol in methanol and heating at 120 °C for 7 days. One difference is that we used strontium acetate as a precursor instead of strontium oxide. Strontium oxide is a high-temperature adsorbent of carbon dioxide (activation energy of 64 kJ/mol

at 800 °C); however, SrO carbonation in temperatures lower than 700 °C is kinetically very slow. To Additionally, SrO is not dissolved in glycerol and methanol, while in our work the formation of Sr^{2+} from strontium acetate dissolution is expected to lead to the formation of strontium carbonate.

CONCLUSIONS

In summary, this research proposes a mechanism for the formation of urchin-like strontium carbonate through glycerolbased solvothermal synthesis in the presence of CO₂. The study highlights that the polymerization of glycerol is a crucial step in shaping the urchin-like morphology, and the presence of dissolved CO₂ redirects the reaction pathway toward the formation of strontium carbonate instead of strontium glycerolate. According to the XRD results, there was a preferred orientation phenomenon and the formation of strontium hydroxide as an intermediate phase. In situ TEM imaging of the precursor solution provides insights into the initial stages of strontium hydroxide formation as an intermediate phase of strontium carbonate synthesis. These images reveal that initially, strontium acetate is soluble in isopropyl alcohol, but as glycerol polymerizes and converts to polyglycerol, the small particles of strontium hydroxide become insoluble in the medium. In addition, SEM images depict that the morphology of the synthesized material changes from sphere to urchin-like with increasing the reaction time. Notably, glycerol plays a vital role in the formation of urchinlike strontium carbonate, as the product of the synthesis without using glycerol was strontium acetate with a plate-like morphology. Overall, the formation of urchin-like strontium carbonate particles is a time-dependent process driven by the polymerization of glycerol and its high reactivity with dissolved CO₂ at elevated temperatures. In our comprehensive DFT study utilizing the VASP and comparing it to experimental results, we discerned a pivotal role of glycerol in facilitating the stable formation of SrCO₃ from CO₂ adsorption on the Sr(OH)₂ surface. Specifically, glycerol likely functions as a coadsorbent or catalyst, enhancing CO2's adsorption energy and guiding its interaction with Sr(OH)₂. Furthermore, the inherently unstable nature of the adsorption of CO2 on Sr(OH)₂ is mitigated in the presence of glycerol. Comparatively, SrCO₃ manifests higher thermodynamic stability, resisting further transformations. AIMD simulations reinforced these findings, indicating glycerol's mediator role without undergoing dissociation on the Sr(OH)₂ surface at elevated temperatures. This research is suggested to significantly contribute to the time-dependent synthesis of urchin-like strontium carbonate by shedding light on the role of glycerol in the process.

ASSOCIATED CONTENT

Supporting Information

The Supporting Information is available free of charge at https://pubs.acs.org/doi/10.1021/acssuschemeng.3c07205.

Thermodynamic data on alkali earth metal oxides carbonation, Gibbs free energy calculations of carbonation process, experimental details, materials, and methods of the research, comparison table outlining conventional synthesis methods for strontium carbonate, additional SEM, TEM, SAED patterns, and XRD information, additional experimental details, materials,

and analysis of zinc glycerolate synthesis, and supplementary DFT information (PDF)

Time-lapsed real-time in-situ GLC TEM data of the formation and growth of strontium hydroxide particles (MP4)

AUTHOR INFORMATION

Corresponding Author

Reza Shahbazian-Yassar — Department of Mechanical and Industrial Engineering, University of Illinois Chicago, Chicago, Illinois 60607, United States; oorcid.org/0000-0002-7744-4780; Email: rsyassar@uic.edu

Authors

Alireza Ghorbani — Department of Mechanical and Industrial Engineering, University of Illinois Chicago, Chicago, Illinois 60607, United States; orcid.org/0000-0002-0738-1040

Vitaliy Yurkiv — Department of Aerospace and Mechanical Engineering, University of Arizona, Tucson, Arizona 85721, United States; Occid.org/0000-0002-3407-891X

Josué M. Gonçalves — Department of Mechanical and Industrial Engineering, University of Illinois Chicago, Chicago, Illinois 60607, United States; Instituto de Química, Universidade de São Paulo, 05508-000 São Paulo, SP, Brazil; ocid.org/0000-0003-0800-077X

Azadeh Amiri — Department of Mechanical and Industrial Engineering, University of Illinois Chicago, Chicago, Illinois 60607, United States

Timothy G. Ritter — Department of Civil & Materials Engineering, University of Illinois Chicago, Chicago, Illinois 60607, United States; orcid.org/0000-0002-5139-1908

Mahmoud Tamadoni Saray — Department of Mechanical and Industrial Engineering, University of Illinois Chicago, Chicago, Illinois 60607, United States

Complete contact information is available at: https://pubs.acs.org/10.1021/acssuschemeng.3c07205

Author Contributions

A.G., J.M.G., and R.S.Y. conceptualized the research and designed the experiments. A.G. and A.A. performed in situ GLC TEM microscopy. T.G.R. performed the XRD characterization. M.T.S. assisted with STEM microscopy. V.Y performed DFT and AIMD simulations and contributed to manuscript writing. A.G., V.Y., J.M.G., and R.S.Y. wrote the manuscript. All authors discussed the results and commented on the manuscript.

Notes

The authors declare no competing financial interest.

ACKNOWLEDGMENTS

This research is partially supported by financial support from the National Science Foundation award DMR-2334386. This work made use of instruments in the electron microscopy core (EMS) of UIC's research resource center (RRC). Also, we extend our sincere appreciation to Fengyuan Shi, the director of EMS core at RRC. V. Yurkiv acknowledges the financial support from NSF award number DMR-2311104. DFT calculations were performed in part using the High-Performance Computing (HPC) resources supported by the University of Arizona TRIF, UITS, and Research, Innovation, and Impact (RII) and maintained by the UArizona Research Technologies department. In addition, the DFT calculations were partially

performed on SDSC Dell Cluster with AMD Rome HDR IB (Expanse) allocation TG-TRA220030 from the Advanced Cyberinfrastructure Coordination Ecosystem: Services & Support (ACCESS) program.

REFERENCES

- (1) Gilbertson, L. M.; Zimmerman, J. B.; Plata, D. L.; Hutchison, J. E.; Anastas, P. T. Designing Nanomaterials to Maximize Performance and Minimize Undesirable Implications Guided by the Principles of Green Chemistry. *Chem. Soc. Rev.* **2015**, 44 (16), 5758–5777.
- (2) Duan, H.; Wang, D.; Li, Y. Green Chemistry for Nanoparticle Synthesis. Chem. Soc. Rev. 2015, 44 (16), 5778–5792.
- (3) Cvjetko Bubalo, M.; Vidović, S.; Radojčić Redovniković, I.; Jokić, S. Green Solvents for Green Technologies. *J. Chem. Technol. Biotechnol.* **2015**, 90 (9), 1631–1639.
- (4) Wolfson, A.; Dlugy, C.; Shotland, Y. Glycerol as a Green Solvent for High Product Yields and Selectivities. *Environ. Chem. Lett.* **2007**, 5 (2), 67–71.
- (S) Prabhavathi Devi, B.; Gangadhar, K. N.; Sai Prasad, P.; Jagannadh, B.; Prasad, R. B. N. A Glycerol-Based Carbon Catalyst for the Preparation of Biodiesel. *ChemSusChem* **2009**, 2 (7), 617–620.
- (6) García, J. I.; García-Marín, H.; Pires, E. Glycerol Based Solvents: Synthesis, Properties and Applications. *Green Chem.* **2014**, *16* (3), 1007–1033.
- (7) Tan, H. W.; Abdul Aziz, A. R.; Aroua, M. K. Glycerol Production and Its Applications as a Raw Material: A Review. *Renewable Sustainable Energy Rev.* **2013**, *27*, 118–127.
- (8) Genç, R.; Clergeaud, G.; Ortiz, M.; O'sullivan, C. K. Green Synthesis of Gold Nanoparticles Using Glycerol-Incorporated Nanosized Liposomes. *Langmuir* **2011**, *27* (17), 10894–10900.
- (9) Zhang, Y. X.; Zhou, X. B.; Liu, Z. L.; Liu, Q. Z.; Zhu, G. P.; Dai, K.; Li, B.; Sun, B.; Jin, Z.; Li, X. H. Green Synthesis of Monodispersed LaCO₃OH Microgears with Novel Plum Blossom-like Structure via a Glycerol-Mediated Solvothermal Method. *RSC Adv.* **2015**, *5* (28), 21925–21930.
- (10) Liu, J.; Ding, F. Nanoporous Materials for Molecule Separation and Conversion; Elsevier, 2020.
- (11) Abbas, S. A.; Iqbal, M. I.; Kim, S. H.; Jung, K. D. Catalytic Activity of Urchin-like Ni Nanoparticles Prepared by Solvothermal Method for Hydrogen Evolution Reaction in Alkaline Solution. *Electrochim. Acta* **2017**, 227, 382–390.
- (12) Vaquero, F.; Navarro, R. M.; Fierro, J. L. G. Influence of the Solvent on the Structure, Morphology and Performance for H₂ Evolution of CdS Photocatalysts Prepared by Solvothermal Method. *Appl. Catal., B* **2017**, *203*, 753–767.
- (13) Lu, F.; Cai, W.; Zhang, Y. ZnO Hierarchical Micro/Nanoarchitectures: Solvothermal Synthesis and Structurally Enhanced Photocatalytic Performance. *Adv. Funct. Mater.* **2008**, *18* (7), 1047–1056
- (14) Wang, B.; Wu, H.; Yu, L.; Xu, R.; Lim, T. T.; David Lou, X. W. Template-Free Formation of Uniform Urchin-like α -FeOOH Hollow Spheres with Superior Capability for Water Treatment. *Adv. Mater.* **2012**, 24 (8), 1111–1116.
- (15) Wei, Z.; Xing, R.; Zhang, X.; Liu, S.; Yu, H.; Li, P. Facile Template-Free Fabrication of Hollow Nestlike α -Fe₂O₃ Nanostructures for Water Treatment. *ACS Appl. Mater. Interfaces* **2013**, 5 (3), 598–604.
- (16) Boyjoo, Y.; Pareek, V. K.; Liu, J. Synthesis of Micro and Nano-Sized Calcium Carbonate Particles and Their Applications. *J. Mater. Chem. A* **2014**, *2* (35), 14270–14288.
- (17) Guo, X. H.; Yu, S. H.; Cai, G. B. Crystallization in a Mixture of Solvents by Using a Crystal Modifier: Morphology Control in the Synthesis of Highly Monodisperse CaCO₃ Microspheres. *Angew. Chem., Int. Ed.* **2006**, 45 (24), 3977–3981.
- (18) Xu, A. W.; Antonietti, M.; Yu, S. H.; Cölfen, H. Polymer-Mediated Mineralization and Self-Similar Mesoscale-Organized Calcium Carbonate with Unusual Superstructures. *Adv. Mater.* **2008**, *20* (7), 1333–1338.

- (19) Yu, J.; Lei, M.; Cheng, B.; Zhao, X. Effects of PAA Additive and Temperature on Morphology of Calcium Carbonate Particles. *J. Solid State Chem.* **2004**, *177* (3), 681–689.
- (20) Ji, X.; Li, G.; Huang, X. The Synthesis of Hollow CaCO₃ Microspheres in Mixed Solutions of Surfactant and Polymer. *Mater. Lett.* **2008**, 62 (4–5), 751–754.
- (21) Bastakoti, B. P.; Guragain, S.; Yokoyama, Y.; Yusa, S. I.; Nakashima, K. Synthesis of Hollow CaCO₃ Nanospheres Templated by Micelles of Poly(Styrene- b -Acrylic Acid- b -Ethylene Glycol) in Aqueous Solutions. *Langmuir* **2011**, 27 (1), 379–384.
- (22) Yu, J.; Guo, H.; Cheng, B. Shape Evolution of SrCO₃ Particles in the Presence of Poly-(Styrene-Alt-Maleic Acid). *J. Solid State Chem.* **2006**, *179* (3), 800–803.
- (23) Sreedhar, B.; Satyavani, C.; Keerthi Devi, D.; Rambabu, C.; Basaveswara Rao, M. V.; Saratchandra Babu, M. Bioinspired Synthesis of Morphologically Controlled SrCO₃ Superstructures by Natural Gum Acacia. *Cryst. Res. Technol.* **2011**, *46* (5), 485–492.
- (24) Xu, Y.; Zhong, X.; Li, Y.; Liu, J. Morphology-Controllable Self-Assembly of Strontium Carbonate (SrCO₃) Crystals under the Action of Different Regulators. *J. Mater. Sci.: Mater. Electron.* **2019**, *30* (24), 21150–21159.
- (25) Gonçalves, J. M.; Ghorbani, A.; Ritter, T. G.; Lima, I. S.; Tamadoni Saray, M.; Phakatkar, A. H.; Silva, V. D.; Pereira, R. S.; Yarin, A. L.; Angnes, L.; Shahbazian-Yassar, R. High-Entropy Metal-Glycerolate as a Precursor Template of Spherical Porous High-Entropy Oxide Microparticles. *J. Colloid Interface Sci.* **2023**, *641*, 643–652.
- (26) Díaz-Álvarez, A.; Cadierno, V. Glycerol: A Promising Green Solvent and Reducing Agent for Metal-Catalyzed Transfer Hydrogenation Reactions and Nanoparticles Formation. *Appl. Sci.* **2013**, *3* (1), 55–69.
- (27) Vitor Braun, J.; Kopp Alves, A. The Role of Glycerol in the Synthesis of Nanomaterials. In *Technological Applications of Nanomaterials*; Kopp Alves, A., Ed.; Springer, 2022; pp 217–228.
- (28) Wang, Z.; He, G.; Yin, H.; Bai, W.; Ding, D. Evolution of Controllable Urchin-like SrCO₃ with Enhanced Electrochemical Performance via an Alternative Processing. *Appl. Surf. Sci.* **2017**, *411*, 197–204.
- (29) Wichannananon, P.; Kobkeatthawin, T.; Smith, S. M. Visible Light Responsive Strontium Carbonate Catalyst Derived from Solvothermal Synthesis. *Catalysts* **2020**, *10* (9), 1069.
- (30) Fang, W.; Ping, H.; Li, X.; Liu, X.; Wan, F.; Tu, B.; Xie, H.; O'Reilly, P.; Wang, H.; Wang, W.; Fu, Z. Oriented Strontium Carbonate Nanocrystals within Collagen Films for Flexible Piezoelectric Sensors. *Adv. Funct. Mater.* **2021**, *31* (45), 1–11.
- (31) Sastry, M.; Kumar, A.; Damle, C.; Sainkar, S. R.; Bhagwat, M.; Ramaswamy, V. Crystallization of $SrCO_3$ within Thermally Evaporated Fatty Acid Films: Unusual Morphology of Crystal Aggregates. CrystEngComm 2001, 3 (21), 81.
- (32) Depner, T. A. Uremic Toxicity: Urea and Beyond. Semin. Dial. **2001**, 14 (4), 246–251.
- (33) Vanholder, R.; Gryp, T.; Glorieux, G. Urea and Chronic Kidney Disease: The Comeback of the Century? (In Uraemia Research). *Nephrol., Dial., Transplant.* **2018**, 33 (1), 4–12.
- (34) Gu, Z.; Xie, H.; Li, L.; Zhang, X.; Liu, F.; Yu, X. Application of Strontium-Doped Calcium Polyphosphate Scaffold on Angiogenesis for Bone Tissue Engineering. *J. Mater. Sci.: Mater. Med.* **2013**, 24 (5), 1251–1260.
- (35) Shi, L.; Du, F. Solvothermal Synthesis of SrCO₃ Hexahedral Ellipsoids. *Mater. Lett.* **2007**, *61* (14–15), 3262–3264.
- (36) Shi, L.; Du, F. Solvothermal Synthesis of Fusiform Hexagonal Prism SrCO₃ Microrods via Ethylene Glycol Solution. *Mater. Res. Bull.* **2007**, 42 (8), 1550–1555.
- (37) Cui, T.; Wu, S.; Zhou, S.; Feng, Q.; Xu, X.; Zhao, H.; Su, Q.; Wang, Y.; Zhao, X.; Yang, Q. Three-Dimensional Microsphere-like Cobalt-Glycerolate Strutted Nickel Hydroxidenitrate Nanoflakes Grown by Hydrothermal Method for Asymmetric Hybrid Supercapacitors. *J. Energy Storage* **2022**, *52* (PA), 104730.

- (38) Sinhamahapatra, A.; Bhattacharjya, D.; Yu, J. Green Fabrication of 3-Dimensional Flower-Shaped Zinc Glycerolate and ZnO Microstructures for p-Nitrophenol Sensing. *RSC Adv.* **2015**, *5*, 37721–37728.
- (39) Zhao, Y.; Huang, Z.; Chang, W.; Wei, C.; Feng, X.; Ma, L.; Qi, X.; Li, Z. Microwave-Assisted Solvothermal Synthesis of Hierarchical TiO₂ Microspheres for Efficient Electro-Field-Assisted-Photocatalytic Removal of Tributyltin in Tannery Wastewater. *Chemosphere* **2017**, 179, 75–83.
- (40) Kim, H.-B.; Jang, D.-J. Morphological Variation of Anatase TiO₂ Crystals via Formation of Titanium Glycerolate Precursors under Microwave Irradiation. *CrystEngComm* **2015**, *17* (17), 3325–3332
- (41) Li, Y.; Yan, X.; Yan, W.; Lai, X.; Li, N.; Chi, Y.; Wei, Y.; Li, X. Hierarchical Tubular Structure Constructed by Mesoporous TiO₂ Nanosheets: Controlled Synthesis and Applications in Photocatalysis and Lithium Ion Batteries. *Chem. Eng. J.* **2013**, 232, 356–363.
- (42) Zhou, L.; Han, Z.; Li, G. D.; Zhao, Z. Template-Free Synthesis and Photocatalytic Activity of Hierarchical Hollow ZnO Microspheres Composed of Radially Aligned Nanorods. *J. Phys. Chem. Solids* **2021**, 148 (August 2020), 109719.
- (43) Yang, L.-X.; Zhu, Y.-J.; Tong, H.; Liang, Z.-H.; Wang, W.-W. Hierarchical Ni(OH)₂ and NiO Carnations Assembled from & DESIGN. *Cryst. Growth Des.* **2007**, *7* (12), 2716.
- (44) The Materials Project. Materials Data on SrCO₃ by Materials Project: United States, 2020.
- (45) Holder, C. F.; Schaak, R. E. Tutorial on Powder X-Ray Diffraction for Characterizing Nanoscale Materials. *ACS Nano* **2019**, 13 (7), 7359–7365.
- (46) Ungár, T. Microstructural Parameters from X-Ray Diffraction Peak Broadening. Scr. Mater. 2004, 51 (8), 777-781.
- (47) Gonçalves, J. M.; Hennemann, A. L.; Ruiz-Montoya, J. G.; Martins, P. R.; Araki, K.; Angnes, L.; Shahbazian-Yassar, R. Metal-Glycerolates and Their Derivatives as Electrode Materials: A Review on Recent Developments, Challenges, and Future Perspectives. *Coord. Chem. Rev.* **2023**, 477, 214954.
- (48) Wang, M.; Jiang, J.; Ai, L. Layered Bimetallic Iron-Nickel Alkoxide Microspheres as High-Performance Electrocatalysts for Oxygen Evolution Reaction in Alkaline Media. *ACS Sustain. Chem. Eng.* **2018**, *6* (5), *6*117–*6*125.
- (49) Bartůněk, V.; Průcha, D.; Švecová, M.; Ulbrich, P.; Huber, S.∴; Sedmidubský, D.; Jankovský, O. Ultrafine Ferromagnetic Iron Oxide Nanoparticles: Facile Synthesis by Low Temperature Decomposition of Iron Glycerolate. *Mater. Chem. Phys.* **2016**, *180*, 272−278.
- (50) Jankovský, O.; Sedmidubský, Ď.; Šimek, P.; Sofer, Z.; Ulbrich, P.; Bartuněk, V. Synthesis of MnO, Mn₂O₃ and Mn₃O₄ Nanocrystal Clusters by Thermal Decomposition of Manganese Glycerolate. *Ceram. Int.* **2015**, *41* (1), 595–601.
- (51) Dong, H.; Feldmann, C. Porous ZnO Platelets via Controlled Thermal Decomposition of Zinc Glycerolate. *J. Alloys Compd.* **2012**, 513, 125–129.
- (52) Hong, J.; Heo, S. J.; Singh, P. Water Mediated Growth of Oriented Single Crystalline $SrCO_3$ Nanorod Arrays on Strontium Compounds. Sci. Rep. 2021, 11 (1), 3368.
- (53) Smeets, P. J. M.; Cho, K. R.; Kempen, R. G. E.; Sommerdijk, N. A. J. M.; De Yoreo, J. J. Calcium Carbonate Nucleation Driven by Ion Binding in a Biomimetic Matrix Revealed by in Situ Electron Microscopy. *Nat. Mater.* **2015**, *14* (4), 394–399.
- (54) Forrester, M.; Becker, A.; Hohmann, A.; Hernandez, N.; Lin, F. Y.; Bloome, N.; Johnson, G.; Dietrich, H.; Marcinko, J.; Williams, R. C.; Cochran, E. RAFT Thermoplastics from Glycerol: A Biopolymer for Development of Sustainable Wood Adhesives. *Green Chem.* **2020**, 22 (18), 6148–6156.
- (55) Salehpour, S.; Dubé, M. A. Reaction Monitoring of Glycerol Step-Growth Polymerization Using ATR-FTIR Spectroscopy. *Macromol. React. Eng.* **2012**, *6* (2–3), 85–92.
- (56) Barros, F. J. S.; Cecilia, J. A.; Moreno-Tost, R.; de Oliveira, M. F.; Rodríguez-Castellón, E.; Luna, F. M. T.; Vieira, R. S. Glycerol

- Oligomerization Using Low Cost Dolomite Catalyst. Waste Biomass Valorization 2020, 11 (4), 1499-1512.
- (57) Salehpour, S.; Dubé, M. A. Towards the Sustainable Production of Higher-Molecular-Weight Polyglycerol. *Macromol. Chem. Phys.* **2011**, 212 (12), 1284–1293.
- (58) Keogh, J.; Tiwari, M. S.; Manyar, H. Esterification of Glycerol with Acetic Acid Using Nitrogen-Based Brønsted-Acidic Ionic Liquids. *Ind. Eng. Chem. Res.* **2019**, *58* (37), 17235–17243.
- (59) Sunder, A.; Hanselmann, R.; Frey, H.; Mu, R. Controlled Synthesis of Hyperbranched Polyglycerols by Ring-Opening Multi-branching Polymerization. *Macromolecules* **1999**, 32, 4240–4246.
- (60) Reinoso, D. M.; Boldrini, D. E. Kinetic Study of Fuel Bio-Additive Synthesis from Glycerol Esterification with Acetic Acid over Acid Polymeric Resin as Catalyst. *Fuel* **2020**, *264* (September2019), 116879
- (61) Xu, Z.; Gong, H.; Chen, M.; Luo, R.; Qian, W.; Peng, Q.; Hou, Z. Catalytic Hydrogenolysis of Glycerol into Propyl Acetate with Ruthenium Complexes. *Catal. Commun.* **2019**, *129* (June), 105743.
- (62) Ionescu, M.; Petrović, Z. S. On the Mechanism of Base-Catalyzed Glycerol Polymerization and Copolymerization. *Eur. J. Lipid Sci. Technol.* **2018**, 120 (6), 1–9.
- (63) Arcis, H.; Zimmerman, G. H.; Tremaine, P. R. Ion-Pair Formation in Aqueous Strontium Chloride and Strontium Hydroxide Solutions under Hydrothermal Conditions by AC Conductivity Measurements. *Phys. Chem. Chem. Phys.* **2014**, *16* (33), 17688–17704
- (64) Ropp, R. C.; Ropp, R. C. Group 16 (O, S, Se, Te) Alkaline Earth Compounds. *Encyclopedia of the alkaline earth compounds*; Elsevier: Oxford, 2013; pp 105–197.
- (65) López-Arce, P.; Gómez-Villalba, L.; Martínez-Ramírez, S.; Álvarez de Buergo, M.; Fort, R. Influence of Relative Humidity on the Carbonation of Calcium Hydroxide Nanoparticles and the Formation of Calcium Carbonate Polymorphs. *Powder Technol.* **2011**, 205 (1–3), 263–269.
- (66) Zhou, W.; Xie, Q.; Li, J.; Zhengwei, C.; Peng, F. Controllable Preparation of Hollow Fibrous SrCO₃. *Bull. Mater. Sci.* **2019**, 42 (1), 12.
- (67) Holm-Jensen, I. A New Gas Absorption Device: Its Application to Titrimetric and Conductometric Micro Determinations of Carbon Dioxide in Air. *Anal. Chim. Acta* **1960**, 23, 13–27.
- (68) Khajeh, M.; Ghaemi, A. Strontium Hydroxide-Modified Nanoclay Montmorillonite for CO₂ Capture: Response Surface Methodology and Adsorption Mechanism. *Int. J. Environ. Anal. Chem.* **2021**, 103 (17), 5311–5336.
- (69) Lisboa, F. d. S.; Silva, F. R. d.; Cordeiro, C. S.; Ramos, L. P.; Wypych, F. Metal Glycerolates as Catalysts in the Transesterification of Refined Soybean Oil with Methanol under Reflux Conditions. *J. Braz. Chem. Soc.* **2014**, 25 (9), 1592–1600.
- (70) Zare Ghorbaei, S.; Ale Ebrahim, H. Carbonation Reaction of Strontium Oxide for Thermochemical Energy Storage and $\rm CO_2$ Removal Applications: Kinetic Study and Reactor Performance Prediction. *Appl. Energy* **2020**, *277* (March), 115604.